Class: Smart Transportation
Students: Souhaiel Ben Salem, Suleyman Barthe-Sukhera
Professors: Olivier Sename, Medero Ariel
Date: January 27, 2022

Longitudinal and Lateral Control of a Vehicle Bicycle-Model

I. Introduction

The number of cars on the road has expanded considerably as a result of the widespread use of automobiles. It therefore becomes increasingly important to consider passenger safety and comfort, fuel consumption optimization, and pollution emission reduction. Automatic control can play a key role in the development of Advanced Driver Assistance Systems to tackle some of these issues (ADAS).

This lab deals with the longitudinal and lateral control of an automotive vehicle within the framework of fully automated guidance. The automotive vehicle is a complicated system with nonlinear longitudinal and lateral coupled dynamics. As a result, automated guidance must be performed in conjunction with longitudinal and lateral control. In this lab, we examine a model predictive control-based automated steering technique. To deal with the longitudinal speed tracking problem, a longitudinal control technique is also proposed. Finally, a unified longitudinal and lateral control strategy helps to improve the combined control performance. This whole control strategy is tested through simulations showing the effectiveness of the present approach.

II. Longitudinal Control

The objective of the longitudinal controller is to have a vehicle track a reference longitudinal velocity. The simplest controller, a purely proportional (P) controller, has the obvious downside to poorly tracking a dynamic reference velocity. In control terms, this means that the vehicle will lag behind reference ramp inputs. Furthermore, neglected system dynamics and forces will cause the P controller to always have a steady-state error. Removing this steady-state error is accomplished by adding an integral term, and thus the minimum complexity controller is defined: a PI controller.

II.I. PI Controller Model

While designing the longitudinal PI controller, there are three factors to consider: minimizing overshoot, ensuring a comfortable experience, and making sure the control is actionable (no over-saturation of any controllers). The generic form of a PI controller is:

$$K = K_p \cdot e(t) + K_I \int e(t)dt \tag{1}$$

The simplified kinematic equations that neglect aerodynamics, road friction, and any external forces is written as:

$$\ddot{x} = \frac{u}{m} \tag{2}$$

Where $\ddot{x}$ is longitudinal acceleration, m is the mass of the vehicle, and u is Force, which is also the control input.

It should be noted that road friction, gravity, and aerodynamic drag forces are included in the MATLAB Simulink simulation, and these forces are defined as follows:

$$F_{aero} = \frac{1}{2}\rho \cdot C_d \cdot A \cdot v^2 \tag{3}$$

Where C_d is the drag coefficient of the vehicle, A, is the effective cross-sectional area of the vehicle, v is the longitudinal velocity, and ρ is the air density, which is a function of altitude defined as:

$$\rho = \frac{p_0\left(1 + \left(\frac{L \cdot Altitude}{T_0}\right)^{9.81 \cdot M/_{R \cdot L}}\right)}{R_{specific} \cdot (T_0 - L \cdot Altitude)}$$

Where $p_0 = 101.325\, kPa$, $T_0 = 288.15\, K$, $L = 0.0065\, K/m$, $M = 0.0289652\, Kg/mol$, $R = 8.31446\, J/(mol \cdot K)$, and $R_{specific} = 287.1\mathrm{J}/(\mathrm{mol} * \mathrm{K})$. For reference, the chosen altitude was 200 meters above sea level.

The longitudinal force due to the vehicle being at an angle (for when the road is not perfectly flat), is defined as:

$$F_{grav} = m \cdot 9.81 \cdot \sin(\theta_1) \tag{4}$$

Where m is the mass of the vehicle, and θ_1 is the angle normal to the road inclination angle along the vehicle's longitudinal axis.

Tire friction forces are modelled as:

$$F_{tire} = C_r \cdot m \cdot 9.81 \cdot \cos(\theta_2) \tag{5}$$

Where C_r is the coefficient of friction of the tire, and θ_2 is the road inclination angle along the vehicle's longitudinal axis.

The necessity of an anti-windup system will be demonstrated in the following section, but the definition of such a controlling mechanism is defined here:

$$K_a = \frac{1}{T_s/_3 + K_I} \tag{6}$$

Where $T_s = 0.01\ sec$ and K_I is the integrator gain from Equation 1.

II.II. PI Controller Performance

Using the simplified equation of system dynamics in Equation 1, a SISO PI controller is designed to have a rise time of ~1 second, and a settling time of ~8 seconds, without too much overshoot. As such, the following proportional and integral gains were used, $K_p = 1500$ and $K_I = 200$.

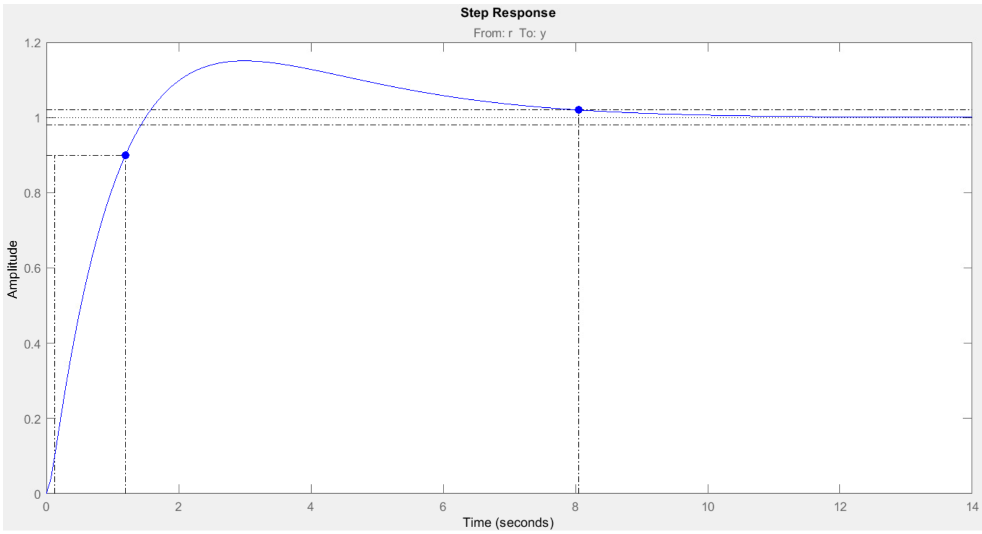

Figure 1: Step Response of PI Longitudinal Controller

It is important to consider controller saturation in all control schemes. Here, the control saturation is assumed to be the physical limitations of road traction, and not any limit on engine torque. The Burckhardt non-linear model of tire friction yields the following force curve with respect to angular velocity of the wheel from a reference longitudinal velocity of $10\ m/s$:

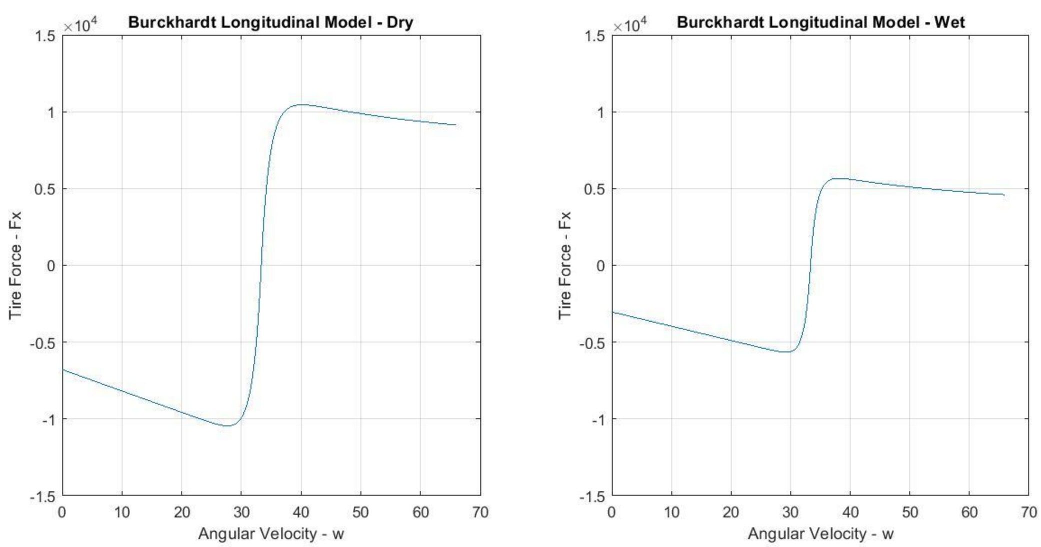

Figure 2: Burckhardt Longitudinal Tire Forces for Dry and Wet Conditions

The saturation limits for longitudinal tire force in dry conditions is defined as: $F_{x,dry} \in [-9000, 9000]N$ and in wet conditions, is defined as: $F_{x,wet} \in [-4000, 4000]N$.

After implementing controller saturation depending on whether the road is dry or wet, it was clear that an anti-windup solution was necessary. As shown in the figure below, the controller saturation is significantly more important when the road is dry, and thus accrues a significant amount of integrator error over time leading to horrific overshooting oscillations.

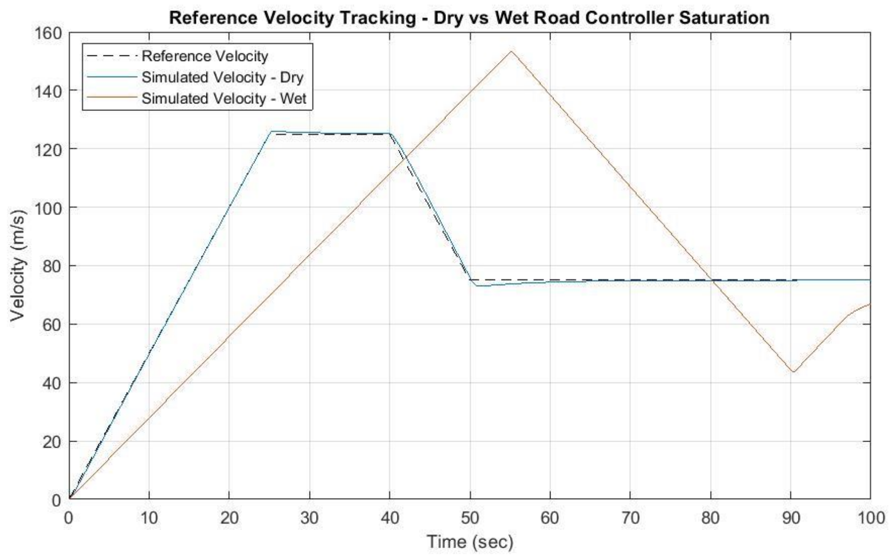

Figure 3: Reference Velocity Tracking of PI Controller in Dry vs Wet Road Conditions

The problem becomes apparent upon inspection of the control output, and the solution is to include an anti-windup feed-back to the PI controller using Equation 6. The same figure from above is recreated below with anti-windup included in the control structure:

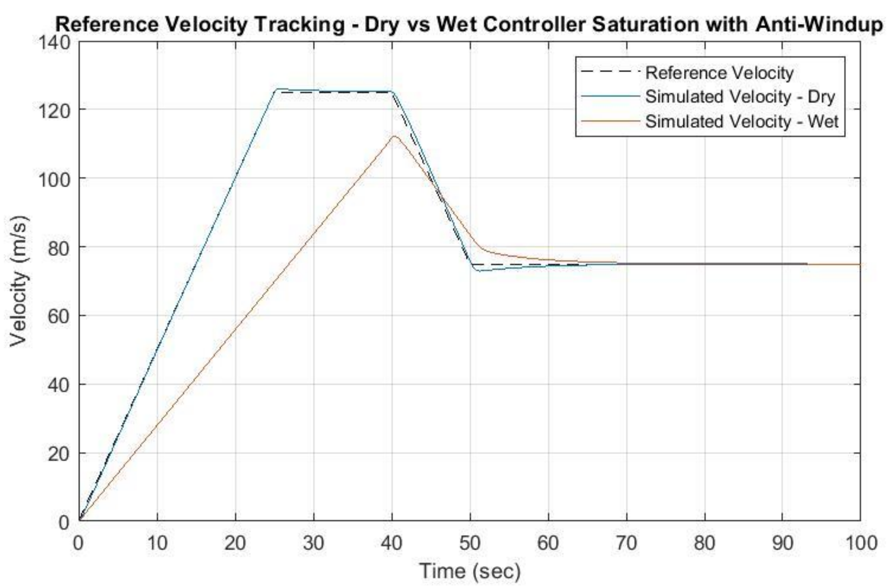

Figure 4: Reference Velocity Tracking of PI Controller in Dry vs Wet Roads with Anti-Windup

III. Lateral Control

The objective of a lateral controller is to adjust the steering angle so that a vehicle follows a refence yaw rate and thus, a refence path. The controller minimizes the current vehicle position and the reference path. In this part we used YALIM, which is a toolbox designed for quadratic programming and optimization, to formulate and solve the MPC optimization problem and eventually implement the closed loop controller.

III.I. MPC Design:

The lateral motion of the vehicle is governed by lateral forces that result from the deformation of the contact patch (surface of contact between the road and tire). These forces are a function of tire slip (α), vertical load applied on the tire (F_z) and friction coefficient (μ)

The lateral forces are modeled using Pacejka's magic formula:

$$F_{ty} = D_y sin\left(C_y . arctan\left(B_y(1 - E_y)\beta + E_y arctan(B_y\beta)\right)\right) e^{(-6|\lambda|^5)} \quad (7)$$

Where $B_y = (2 - \mu)b_y$, $C_y = (5/4 - \mu/4)c_y$, $D_y = d_y\mu$ and $E_y = e_y$ are the lateral parameters function of $\mu \in [0; 1]$. Additionally, the tire/road adhesion coefficient "$e^{(-6|\lambda|^5)}$" is used to model the lateral friction forces dependency w.r.t. the slip ratio: when slipping occurs on a wheel, lateral forces are reduced.

The planar bicycle model (Dugoff et al) was used to derive the main dynamics under interest, which are:

- Equation of lateral motion:

$$mv(\dot{\beta} + \dot{\psi}) = F_{yf} + F_{yr} \quad (8)$$

- Equation of yaw motion:

$$I_z\ddot{\psi} = l_f F_{yf} - l_r Fyr \quad (9)$$

From these equations the simplified 2-DOF is defined as

$$\begin{bmatrix} \ddot{\psi} \\ \dot{\beta} \end{bmatrix} = \begin{bmatrix} -\frac{l_f^2 C_f + l_r^2 C_r}{I_z v} & \frac{l_r C_r - l_f C_f}{I_z} \\ -1 + \frac{l_r C_r - l_f C_f}{mv2} & -\frac{C_f + C_r}{mv} \end{bmatrix} \begin{bmatrix} \dot{\psi} \\ \beta \end{bmatrix} + \begin{bmatrix} \frac{l_f C_f}{I_z} \\ \frac{C_f}{mv} \end{bmatrix} \delta^*$$

While designing the MPC controller, there are two considerations to keep in mind: the evolution of the vehicle's dynamics and the forces acting on the tires defined previously. This is why we defined two constraints:

- Equality constraint i.e., dynamic constraint, which is basically a one-step-ahead prediction function:

$$X(k+1) = A_d X(k) + B_d u(k) \tag{10}$$

Where A_d and B_d are discretized matrices derived from A and B.

- Inequality constraint:

$$-60 * \pi/180 \leq u(k) \leq 60 * \pi/180 \tag{11}$$

We define our quadratic objective function as:

$$objective = (r - C * x(k)' * Q * (r - C * x(k)) + u(k) * R * u(k) \tag{12}$$

Where r is the reference, $C = [1\ 0]$ is a matrix used to extract the first state variable ($\dot{\psi}$), R and Q are the weighting matrices.

<u>III.II. Explicit SS MPC and Implicit MS MPC</u>

In a first step, we Implemented a simple MPC using a single shooting strategy, where we only consider the control sequence $\boldsymbol{u}$ over the prediction horizon $\boldsymbol{N = 10}$. We also added the initial state ($\mathbf{X_0}$) as a decision variable to avoid reformulating the problem every time we have a new initial state. This also enable us to obtain a solution from an arbitrary initial state (i.e., initial yaw rate $\boldsymbol{\dot{\psi}}$ and side slip angle $\boldsymbol{\beta}$).

The optimization problem generated by the precedent formulation is a problem in the control variables (and initial state). However, it is move convenient to optimize over both the control and state vectors and model the system dynamics using equality constraints.

For a randomly picked initial state and weighting matrices $Q = 5$ and $R = 9$ and a constrained control vector ($-\frac{\pi}{3} \leq \mathrm{u} \leq \frac{\pi}{3}$<), we get the following optimal sequences for each formulation:

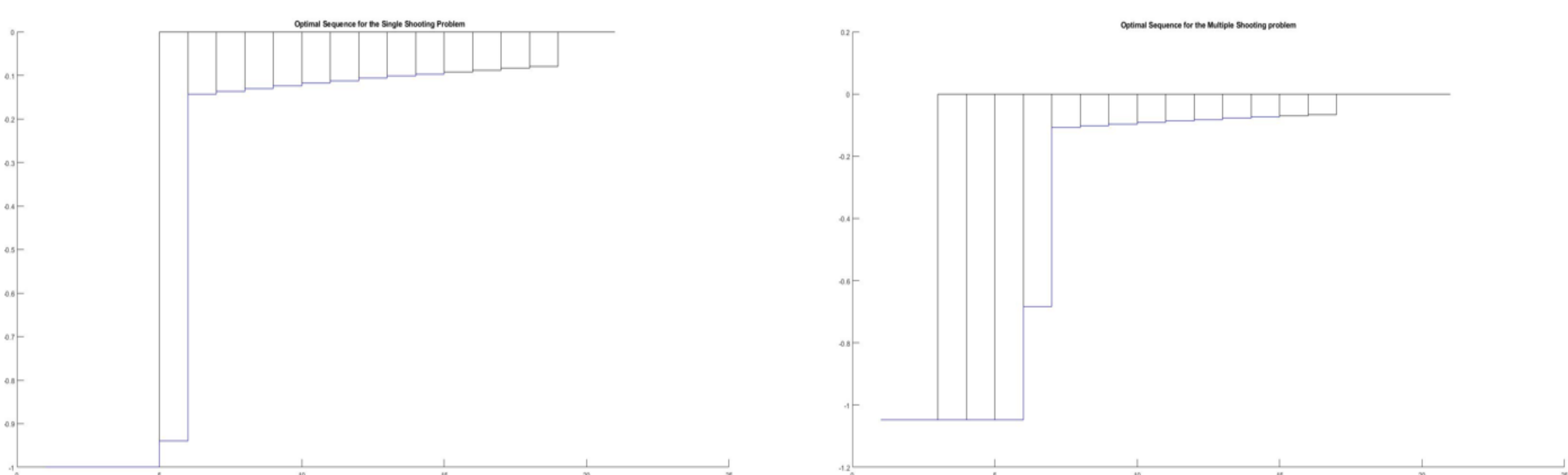

Figure 5: Optimal control sequence for both SS and MS MPC formulations

III.II. Closed-Loop Nonlinear MPC

In this part we apply our MPC controller (using the MS strategy) to the nonlinear model of the lateral vehicle le dynamics to make the system adhere to a specific (reference) longitudinal velocity $\boldsymbol{Vx} = \boldsymbol{R}.\boldsymbol{w}$ (which can vary over time) and yaw rate $\dot{\psi} \;= 0.15\, rad/sec$.

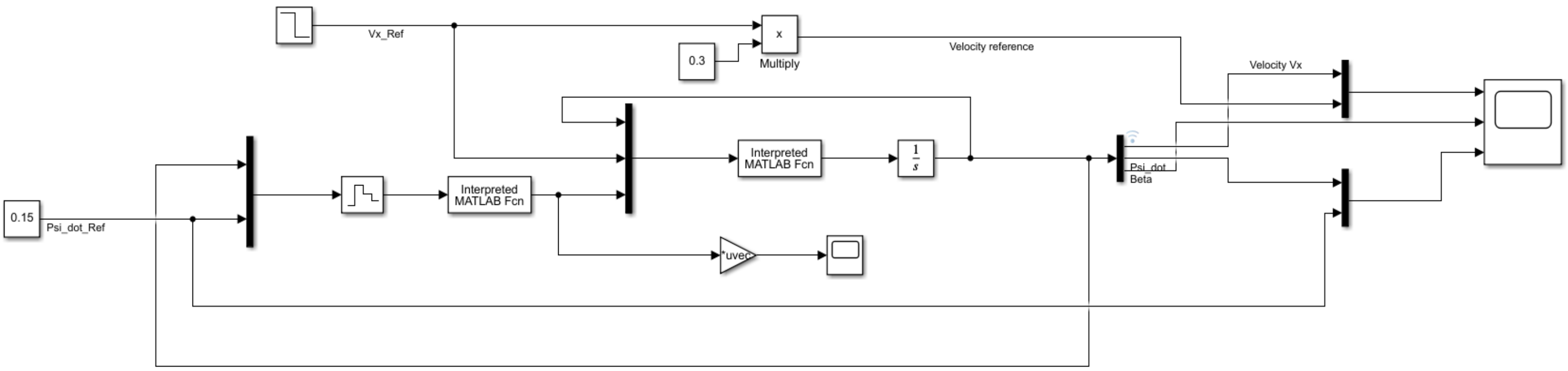

Figure 6: The stand-alone MPC controller

The MPC controller's performance depends on the weighting matrices Q and R. To find the best values for these matrices this, a simple tuning strategy can be followed where we fix the value of one matrix and change the value of the other until there is no significant performance improvement. Afterwards, we can tune the other matrix using the same principle.

Henceforth, the following weighting matrices were used**:** $\boldsymbol{Q} = \mathbf{10}$ and $\boldsymbol{R} = \ \mathbf{2}$ **(**which means that we are putting much more weight on reference tracking than on input regulation**)**, along with a sampling period $\boldsymbol{Ts} = \mathbf{0.01}$ and a prediction horizon $\boldsymbol{N} \;= \mathbf{10}$.

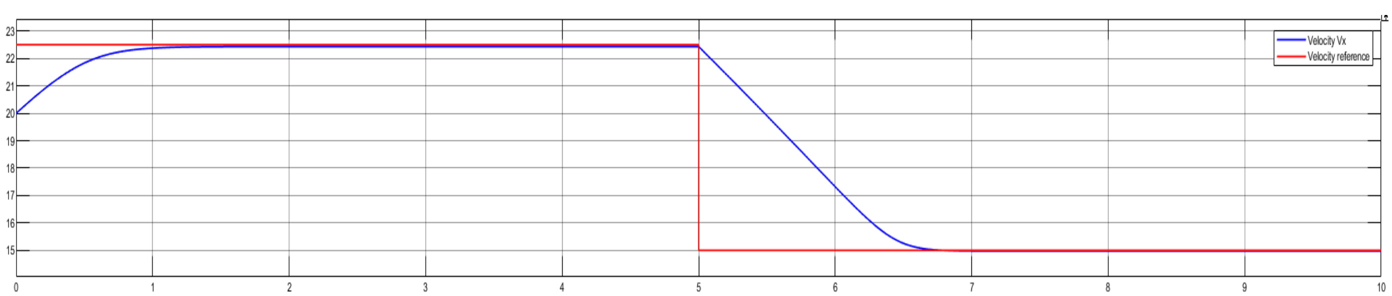

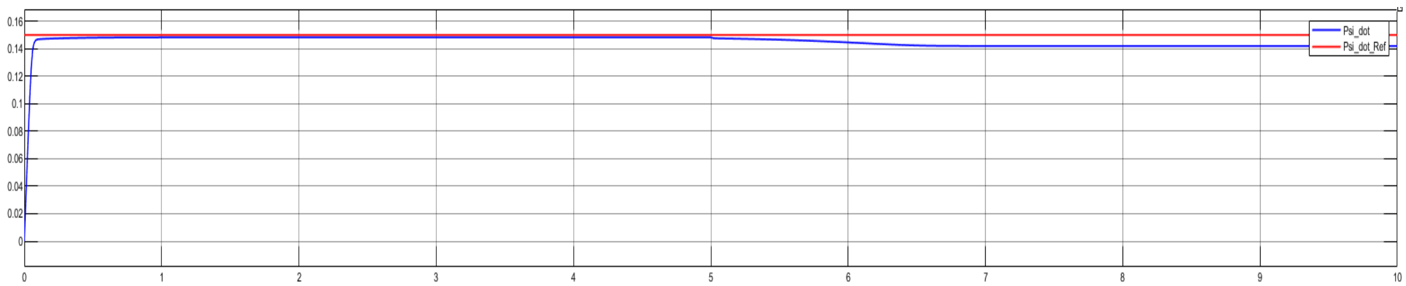

Figure 7: Reference velocity and yaw rate tracking

We were able to converge to the reference velocity $\boldsymbol{Vx_{ref}}$ after **1 second** at the start and **1.5 seconds** following the drop of the reference velocity from **22.5 m/s** to **15 m/s.** we were also able to converge to the reference yaw rate $\dot{\boldsymbol{\psi}}$ after **0.2 seconds** without overshooting the reference value.

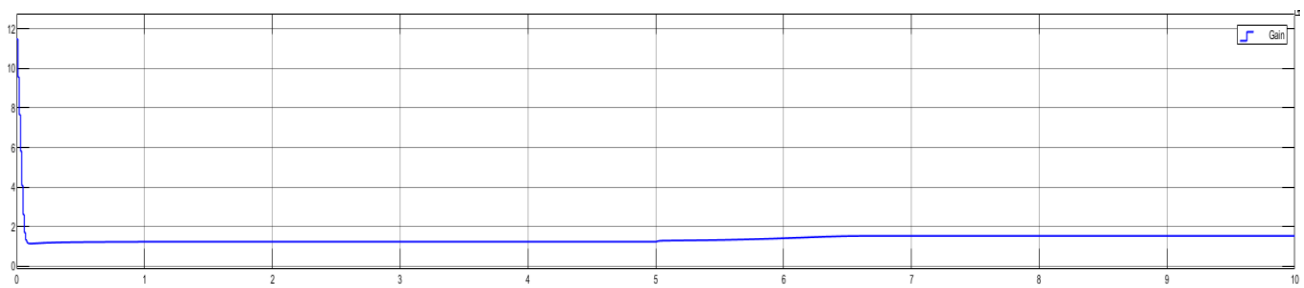

Figure 8: The optimal sequence (steering angle)

The figure above shows the MPC's control action. The controller applies the first control in the optimal sequence until the next sampling instant and at the new reached state, formulate the new problem and solve it to get the new best sequence of actions, apply the first control in this new sequence and so on. We can see that starting from an initial guess of the steering angle **δ=11.8,** the controller was able to generate an optimal control trajectory that satisfies the constraints and leads to the desired yaw rate and longitudinal velocity**.**

IV. Full Dynamics and Trajectory Tracking

The objective of this part is to assess the performance of our control scheme i.e., the combined later and longitudinal controllers when performing in a realistic scenario like trajectory tracking.

The trajectory to be followed is simple racetrack:

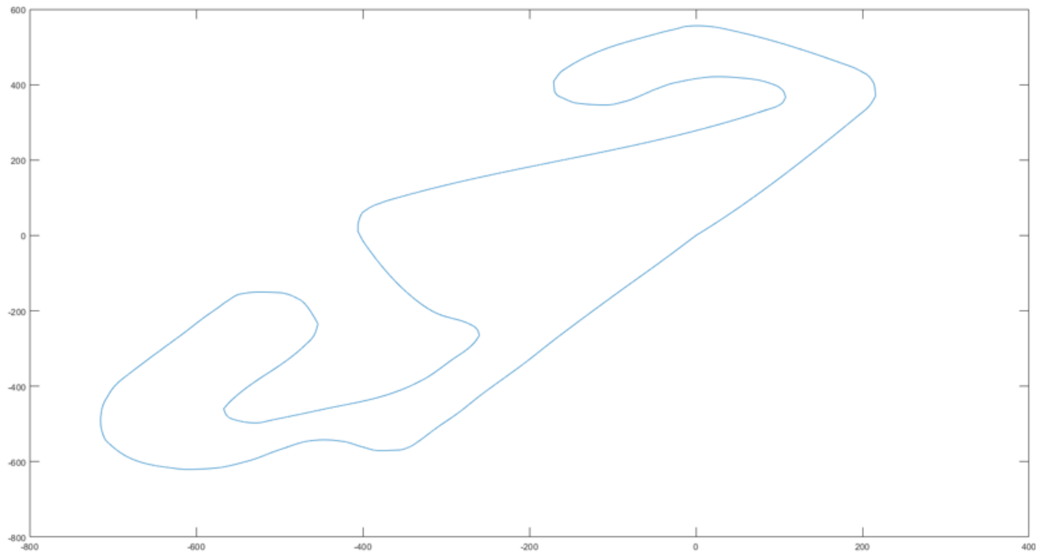

Figure 9: The reference trajectory

For this purpose, we used the **Pure Pursuit** algorithm, which takes in the reference the current position of the vehicle, its side slip angle and linear speed and produces a reference yaw that when followed, keeps the vehicle on the desired path. This reference yaw rate will be the input for the MPC controller.

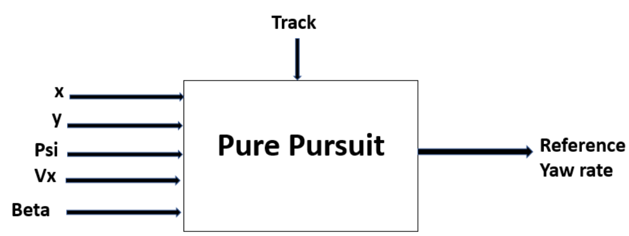

Figure 10: Pure pursuit illustration

<u>IV.I. Combined PI and MPC Controller</u>

The reference velocity, obtained as a piece-wise function dependent on the position of the vehicle in the track, is fed to the PI controller, for longitudinal control. The control output of the PI controller, reference wheel rotation rate, is passed to the MPC controller for yaw control. Combining the two yields a Simulink schema as shown below:

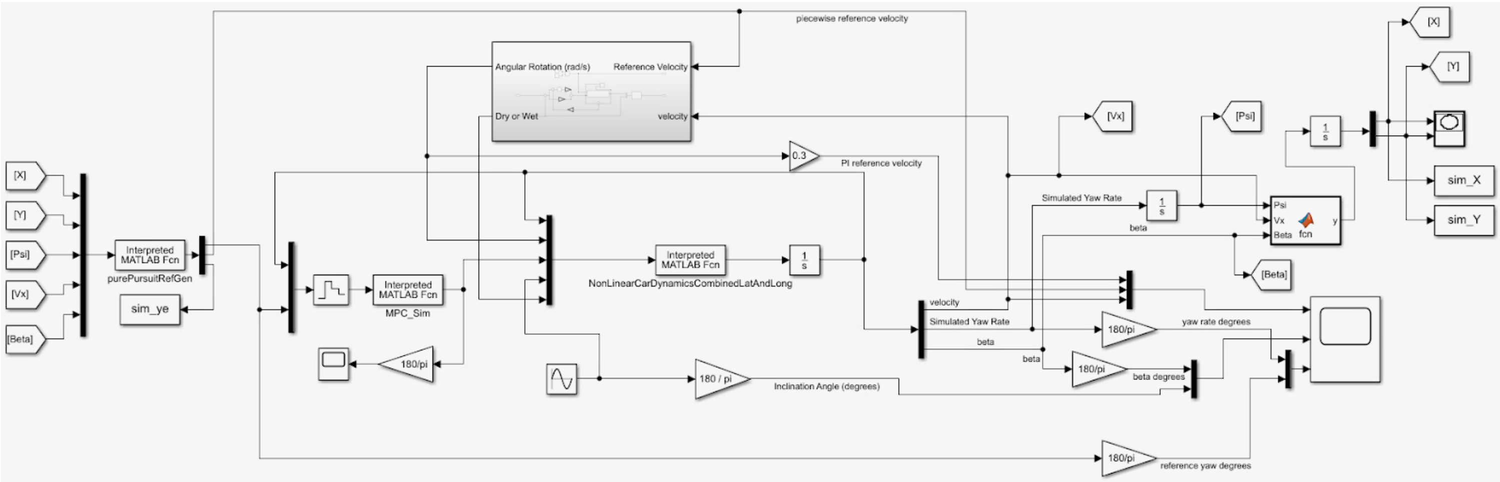

Figure 11: Unified PI and MPC Controller

IV.II. Performance Analysis – Constant Velocity

To assess the performance of our combined controller, we tackled the trajectory following task using different constant velocities across the whole trajectory for each test.

1. 50km/h:

When tested with a refence velocity of $50 km/h$, our controller performed well and the vehicle was able to follow the refence yaw rate and refence velocity almost immediately. This is also reflected on the vehicle trajectory w.r.t refence trajectory.

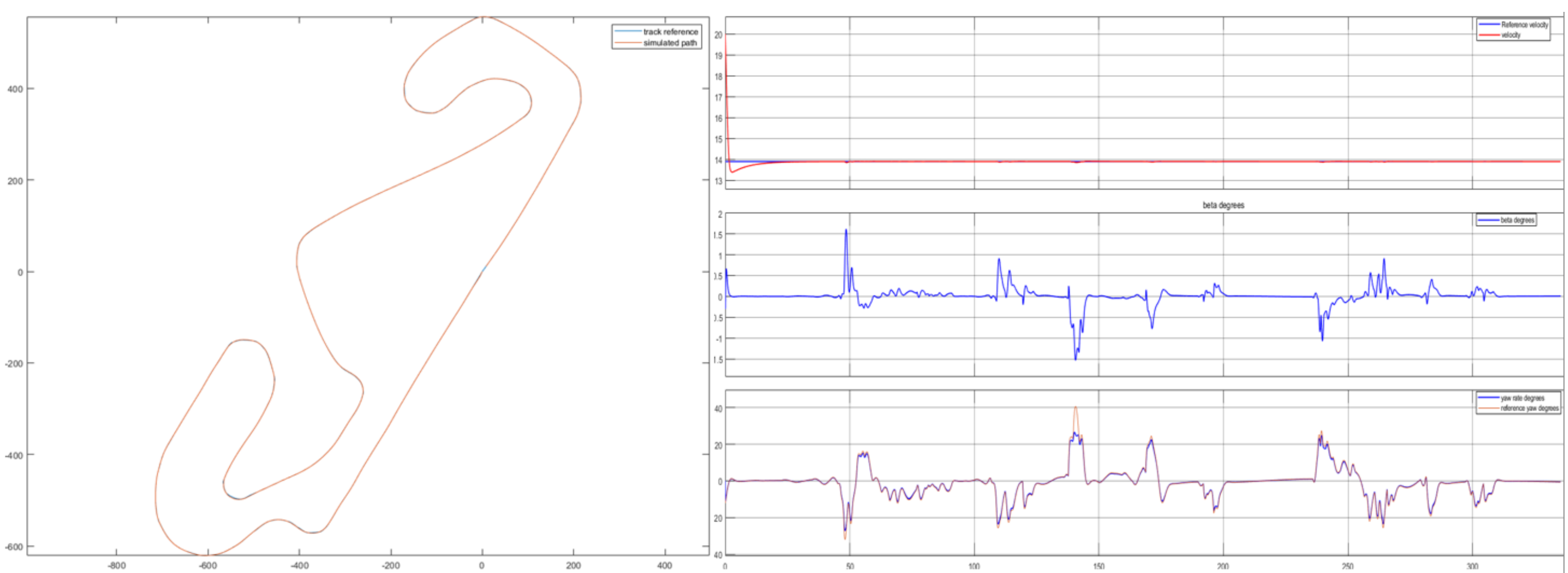

Figure 12: Results obtained for Vx=50km/h

2. <u>75km/h:</u>

When operating at a higher speed, we begin to see the limitations of our controller as the vehicle is unable to keep up with the reference yaw rate. In fact, we see that the reference yaw is much higher that the vehicle's when performing a turn. This means that the vehicle would go off-track when trying to make almost every turn. This problem is caused by the increase of the look-ahead distance which varies proportionally with Vx.

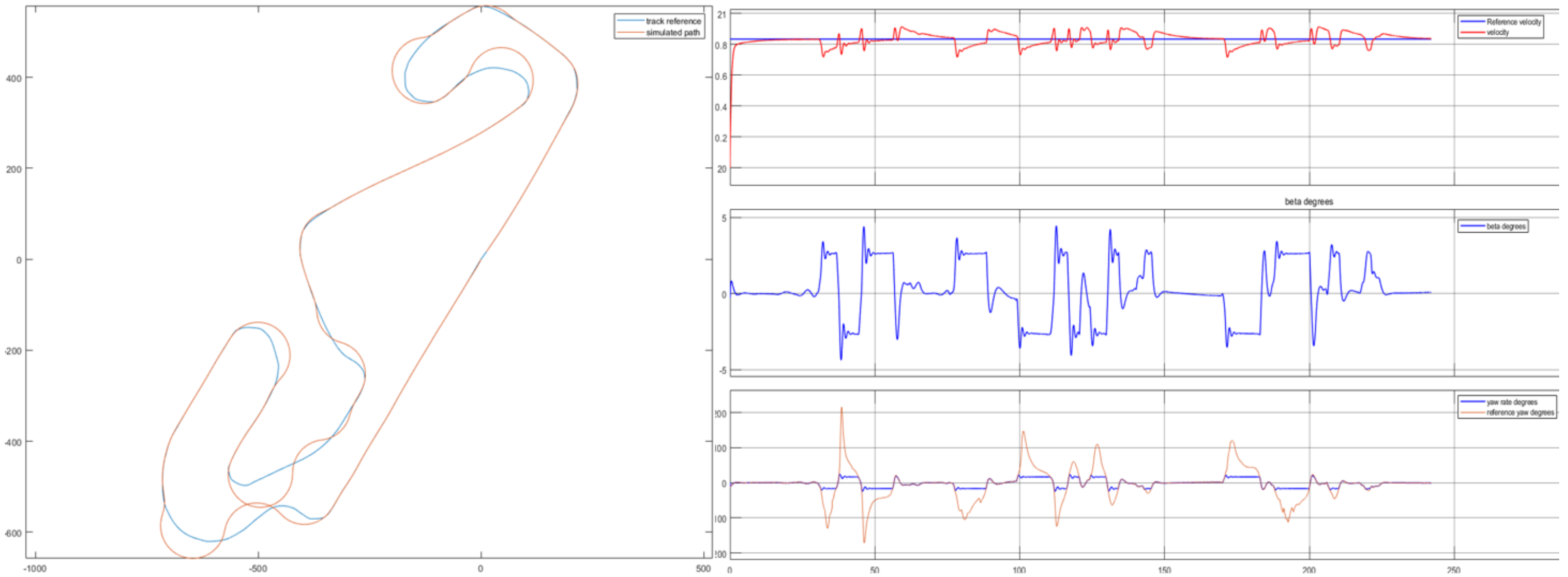

Figure 13: Results obtained for Vx=75km/h

3. <u>90km/h:</u>

When we increase the reference velocity to $90km/h$, all the problems mentioned before get amplified.

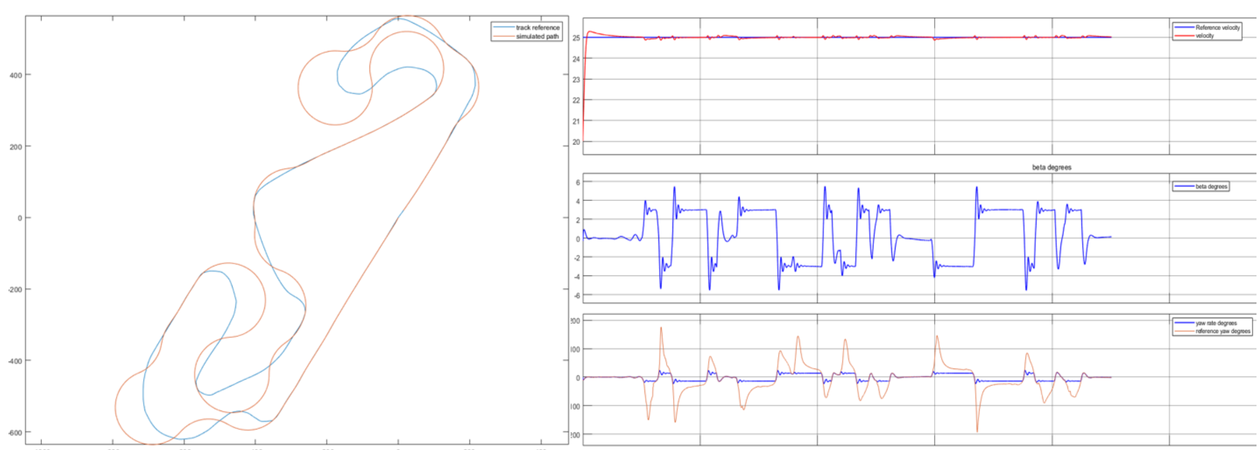

Figure 14: Results obtained for Vx=90km/h

IV.III. Performance Analysis – Variable Velocity

The previous tests suggest that a correction needed to be made in order to improve the controller's performance. The first logical idea that comes to mind is to decrease the lookahead distance. In order to quickly regain the path between waypoints, a small lookahead distance will the vehicle to move quickly towards the path. However, as can be seen in the figure below, the vehicle overshoots the path and oscillates along the desired path.

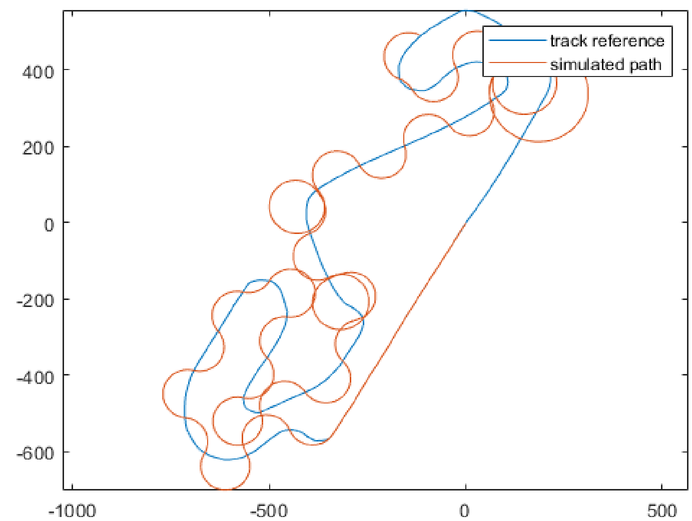

Figure 15: Results obtained for Vx=75km/h and a small lookahead distance

The solution is to use an adaptive reference velocity i.e., different $V_{x_{ref}}$ values for different sections of the reference trajectory as we want to accelerate as much as possible for straight potions of the track and brake when making a turn.

This strategy improved the controller's performance significantly and the time needed to complete the whole track was reduced to **~250 seconds.**

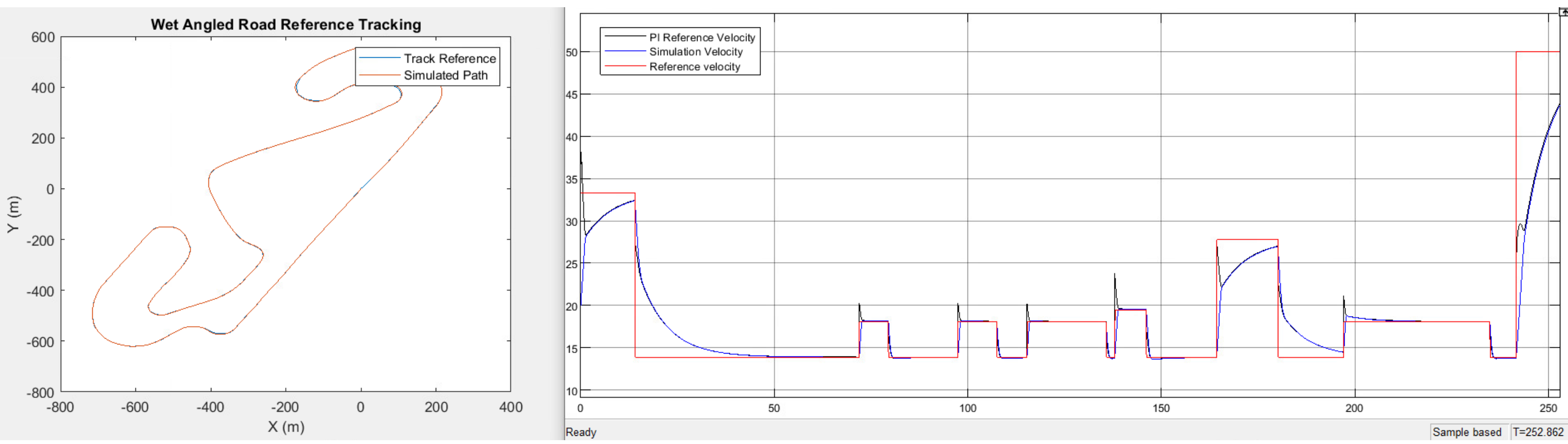

Figure 16: Trajectory and velocity tracking

IV.IV. Performance Analysis – Suboptimal Driving Conditions

It is interesting to compare the performance of the combined PI and MPC controller when the road conditions are less than optimal. The results from all previous tests, Figures 12 – 16, assume the road is perfectly flat and dry. Here, two alternate scenarios are simulated: first is a wet, but flat, road, and second is a wet and variably inclined road. The wet condition influences the PI controller as previously mentioned in Section II, but also influences the MPC controller. Using the same piece-wise velocity reference generator as a function of track position, the first (wet only) scenario yields the following result:

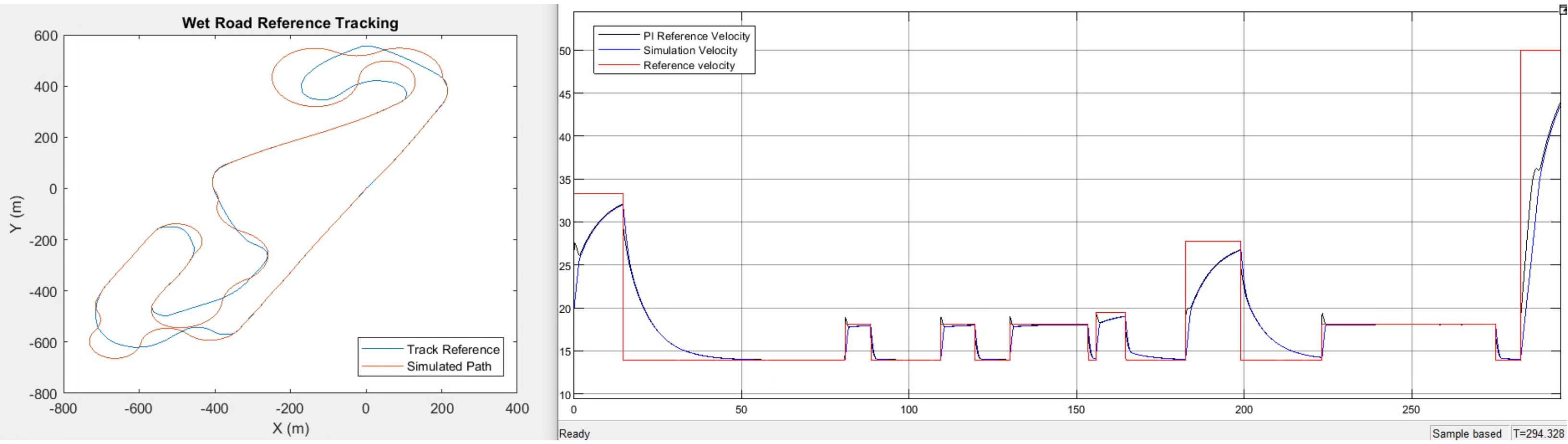

Figure 17: Wet Flat Road

While this follows the same piecewise velocity reference, the acceleration and deceleration are significantly impacted by the wetness of the road. The significant increase in trajectory overshoot is due in part to the vehicle's inability to slow down fast enough before a curve, but also by the physical constraints of the MPC controller to keep the vehicle controllable.

The second scenario entails both a wet road as well as a road inclination angle which oscillated as a function of time (1 oscillation/minute):

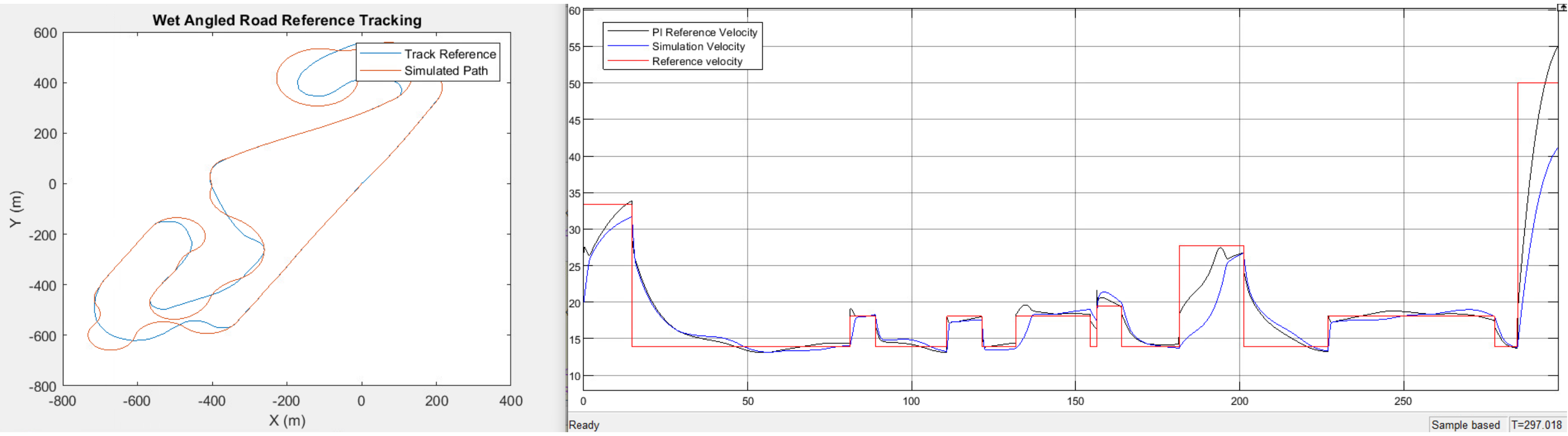

Figure 18: Wet Oscillating Road

V. Conclusion

The combination of longitudinal and lateral control is effectively accomplished by combining an anti-windup PI controller with an MPC controller for longitudinal and lateral control respectively. The performance of this combination of controllers is tested on a simulated Montmelo F1 racetrack where the vehicle accelerates to a top speed of 150 kph and appropriately decelerates to follow the turns of the track smoothly and safely. The impact of driving strategy (constant velocity compared to piecewise velocity) is demonstrated in Figures 12 – 15, and the importance of driving conditions is demonstrated in Figures 17 and 18. With an optimal driving condition and a piecewise reference velocity as a function of position on the racetrack, the simulated vehicle achieves a lap time of about 250 seconds. A Formula 1 vehicle can complete a lap in about 78 seconds, and this three-fold decrease in circuit time can be explained by the vehicles ability to accelerate to ~ 100km/h in just over 2.6 seconds, whereas the simulated vehicle can accelerate to this velocity in roughly 10 seconds, and the fact that the simulated vehicle began in the middle of the straight-away at significantly less than maximum velocity.

In conclusion, the unified longitudinal and lateral controller provides satisfactory control of the vehicle within reasonable and safe limits of operation. Suggestions for future work include identifying and simulating the effect of road bank angle in addition to road inclination angle. This is expected to play a significant role in how fast the vehicle can turn. Another perspective of where research could continue is by improving the PI controller to consider a chain of vehicles ahead of it. By using the latest technology in vehicle-to-vehicle communication, accidents due to traffic jams could be avoided and would integrate nicely with the string stability control perspective.